

Serial Analysis of Gene Expression in the Corneal Endothelium of Fuchs' Dystrophy

John D. Gottsch,¹ Amanda L. Bowers,¹ Elliott H. Margulies,² Gerami D. Seitzman,¹ Sean W. Kim,¹ Saurabh Saha,³ Albert S. Jun,¹ Walter J. Stark,¹ and Sammy H. Liu¹

PURPOSE. To compare the gene expression profiles of normal human corneal endothelium with Fuchs' corneal endothelium, by using serial analysis of gene expression (SAGE).

METHODS. Three pairs of normal human corneas were obtained from eye banks. Thirteen bisected Fuchs' corneal buttons were processed at the time of corneal transplantation. The endothelia of normal and Fuchs'-affected corneas were stripped, and total RNA was isolated. Serial analysis of gene expression (SAGE) was performed to identify and quantify gene transcripts. Genes over- and underexpressed by Fuchs' endothelium were limited to $P < 0.01$ by the method of Audic and Claverie.

RESULTS. A total of 19,136 tags were identified with 9,530 from normal and 9,606 from Fuchs' endothelium. The expression of 18 transcripts was upregulated, and 36 transcripts were downregulated in Fuchs' endothelium compared with normal tissue. Upregulated transcripts included serum amyloid A1 and A2, metallothionein, and apolipoprotein D. Of the downregulated transcripts, 26 matched known genes, 3 matched expressed sequence tags (ESTs), and 7 were unknown to current databases. One downregulated transcript involved a newly reported bicarbonate transporter. Decreased transcripts related to antioxidants and proteins conferring protection against toxic stress were noted in Fuchs' versus normal endothelium including nuclear ferritin, glutathione *S*-transferase- π , and heat shock 70-kDa protein. Nine different SAGE tags matching mitochondrial sequences accounted for 25% of the ESTs that were decreased in Fuchs' endothelium.

CONCLUSIONS. SAGE analysis comparing normal to Fuchs' endothelium demonstrates diminished expression of mitochondrial, pump function, and antiapoptotic cell defense genes. (*Invest Ophthalmol Vis Sci.* 2003;44:594-599) DOI:10.1167/iovs.02-0300

Fuchs' dystrophy is a bilateral, slowly progressive primary disease of the corneal endothelium characterized by enlarged, irregular endothelial cells (cornea guttata) and focal areas of thickened Descemet's membrane.^{1,2} Fuchs' dystrophy is inherited as an autosomal dominant trait and in its expression has been reported to be more severe in women than

men.³⁻⁵ Early studies have found differences in pump function, in aqueous humor composition, and in the Descemet's membrane proteins in Fuchs' compared with normal endothelium. The etiology of Fuchs' endothelial dystrophy is unknown, but a gene mutation is strongly suspected. A systematic determination of gene expression profiles in Fuchs' compared with normal corneal endothelium may shed light on the underlying genetic defect responsible for this disease.

The functional activities of a specific cell are characterized by a set of expressed genes (the transcriptome). Pathologic changes in cell function can be associated with alterations of gene expression patterns where identification of differentially expressed genes can be useful to recognize disease processes. For example, genes exhibiting the greatest difference in expression between normal and diseased endothelium are likely to be relevant to the disease processes. Currently, oligonucleotide or cDNA microarrays^{6,7} and serial analysis of gene expression (SAGE)⁸⁻¹⁰ are the techniques most commonly used to compare global gene expression profile changes in normal or diseased tissues. One difference between these two technologies is that a microarray is limited to a finite number of gene sequences localized to the chip. However, SAGE allows the generation of expressed sequenced tags (ESTs), which are solely dependent on gene expression in the tissue. This allows for the identification of novel genes expressed in a given tissue. SAGE has the additional advantage of providing quantitative information about the level of gene expression.⁸⁻¹⁰ SAGE depends on the generation of short sequence tags at a specific location within a transcript. These tags, which contain sufficient information to identify a gene uniquely, are generated, concatenated, and sequenced. By identifying corresponding genes for each tag and tabulating the frequency for generating each tag, the number of genes expressed and their expression level can be estimated. In the present study, we used SAGE to analyze the differences in gene expression between normal endothelium and endothelium from Fuchs' dystrophy.

MATERIALS AND METHODS

Fuchs' Corneal Specimens

Fuchs' dystrophy corneal buttons from 13 patients were obtained from bisected pathologic specimens immediately after removal for penetrating keratoplasties. Bisected corneal buttons were transported immediately to the laboratory where the endothelium and Descemet's membrane were peeled immediately from the stroma and stored in liquid nitrogen until use. The mean age of the 13 patients, eight of whom were women, was 72 ± 8 years.

Generation of SAGE Libraries

The Fuchs' SAGE library was constructed according to the SAGE protocol⁸ (available at http://www.sagenet.org/sage_protocol.htm), provided in the public domain by the Johns Hopkins Oncology Center, Molecular Genetics Laboratory, Baltimore, MD. The normal SAGE library was constructed as previously described.⁹

SAGE Data Analysis

All sequence data were analyzed with the *Pbred* base-calling algorithm.¹¹ The eSAGE ver. 1.2a computer program (<http://research.nhgri>

From the ¹Center for Corneal Genetics, Cornea and External Disease Service, The Wilmer Eye Institute, Baltimore, Maryland; the ²Genome Technology Branch, National Human Genome Research Institute, National Institutes of Health, Bethesda, Maryland; and ³The Johns Hopkins Oncology Center Molecular Genetics Laboratory, The Johns Hopkins School of Medicine, Baltimore, Maryland.

Supported in part by a RPB Physician/Scientist Award (JDG) and by the Stavros Niarchos Foundation (WJS).

Submitted for publication March 29, 2002; revised May 15, 2002; accepted May 23, 2002.

Commercial relationships policy: N.

The publication costs of this article were defrayed in part by page charge payment. This article must therefore be marked "advertisement" in accordance with 18 U.S.C. §1734 solely to indicate this fact.

Corresponding author: John D. Gottsch, The Wilmer Eye Institute, Johns Hopkins Hospital, 600 N. Wolfe Street, Maumenee #321, Baltimore, MD 21287; jgottsch@jhmi.edu.

TABLE 1. Summary of the SAGE Libraries

| | Normal | Fuchs' | Combined |
|---------------------------------------|--------|--------|------------|
| Combined SAGE tags excluding linkers* | 9,530 | 9,606 | 19,136 |
| Unique transcripts | 4,724 | 5,258 | 8,978 |
| Transcripts unique to each library | 3,720 | 4,254 | |
| Transcripts common to both | | | 1004 |
| Linker contamination | 7 | 269 | 276 (1.4%) |

* SAGE tags were extracted from the *Pbred*-analyzed sequence data (*.phd.1 files) using eSAGE v1.2, so that sequences containing base calls with *Pbred* quality values less than 20 (error rate of 1%) were not added to the database.

nih.gov/eSAGE/, provided in the public domain by the National Human Genome Research Institute [NHGRI], National Institutes of Health, Bethesda, MD) was used to extract and analyze the SAGE data.¹² SAGE tags were extracted from high-quality sequence data by analyzing the *Pbred*-generated PHD-formatted output files (*.phd.1) with eSAGE, which was programmed to exclude automatically the sequences with *Pbred* quality values less than 20. Analysis of SAGE tag GC content was performed as described in Margulies et al.¹³

Statistical Tests for Identifying Differentially Expressed SAGE Tags

Before determining whether specific pair-wise differences exist between the two populations of SAGE tags, a formal statistical test was used to validate an overall difference between the normal and Fuchs' data sets. Because the χ^2 test of independence performs poorly when tag counts are less than five,¹⁴ a Monte Carlo simulation approach was used to determine the overall difference between the two populations of SAGE data.¹⁵ This overall test was also used to determine the

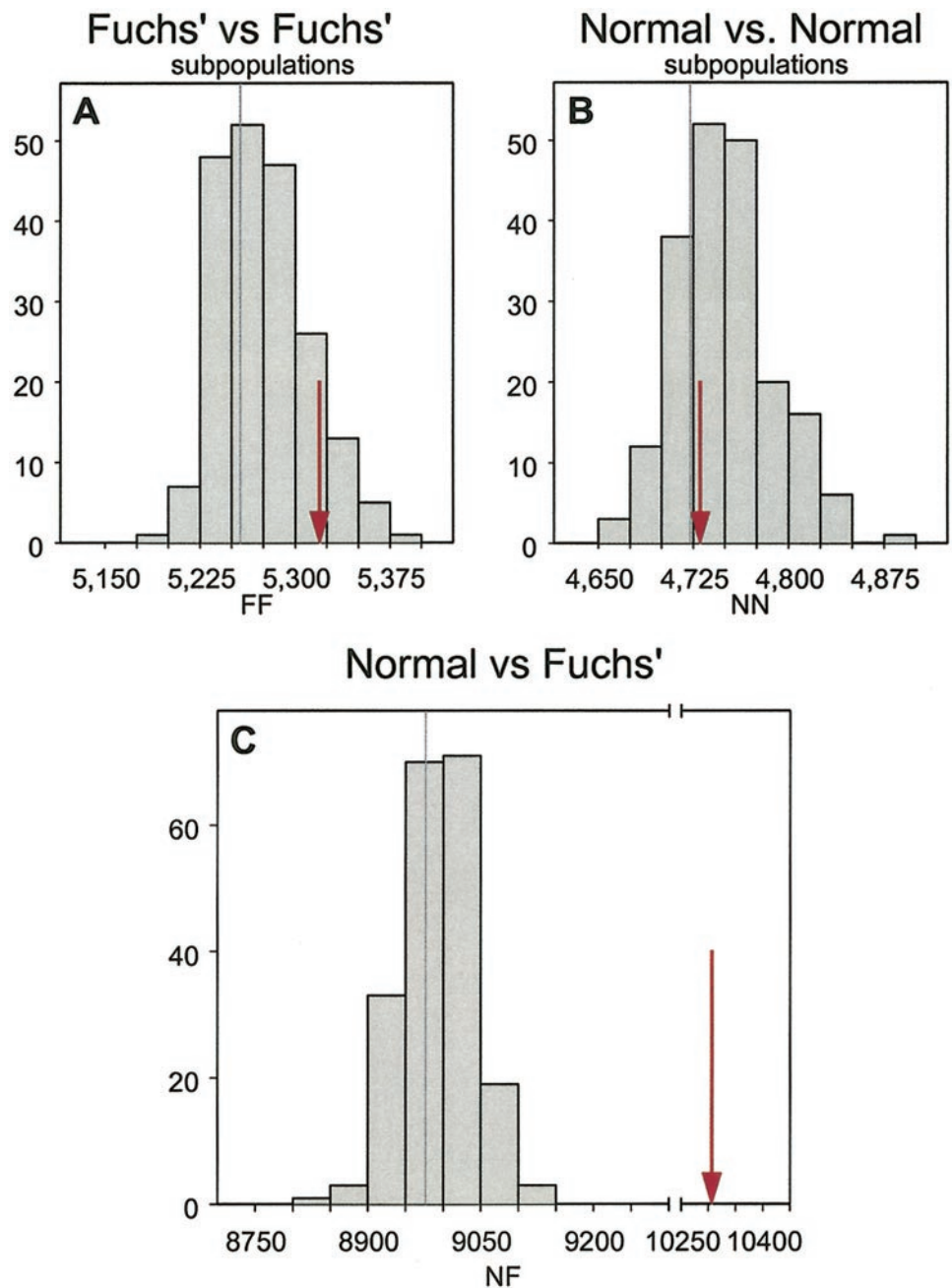


FIGURE 1. Test for overall difference between two populations of SAGE data. Histograms showing the distribution of χ^2 statistics under the null hypothesis of no difference. Distributions were generated from 200 Monte Carlo simulations between subpopulations of Fuchs' SAGE data (A), between subpopulations of normal SAGE data (B), and between the normal and Fuchs' data (C). Red arrow: observed χ^2 value. Subpopulations of SAGE data from the same library have observed χ^2 data that fall within the null distribution (A, B), indicating that these SAGE libraries are reproducible. (C) The observed χ^2 value fell outside the null distribution, indicating an overall difference between the normal and Fuchs' SAGE libraries.

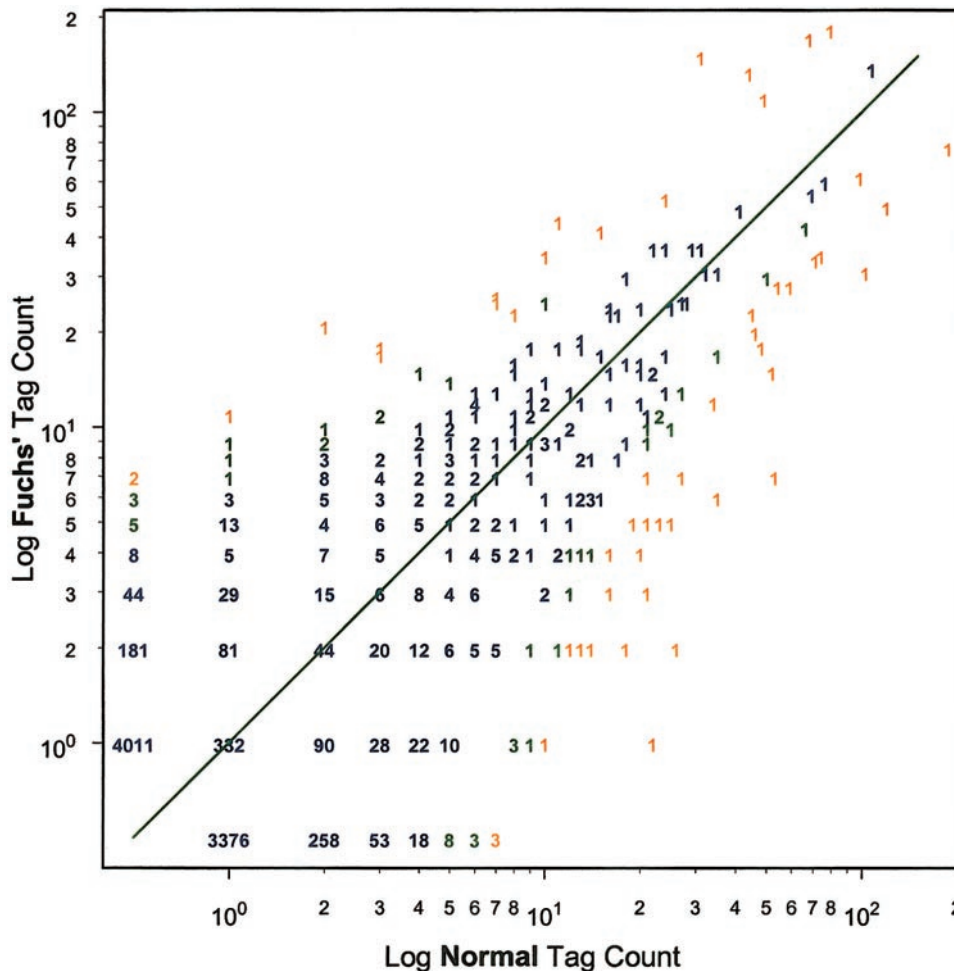


FIGURE 2. Scatterplot of tag abundance distributions in the normal and Fuchs' SAGE libraries. Note the log scale. Each point represents a tag with a given frequency in the normal (x-axis) and Fuchs' (y-axis). The number at each point indicates the number of unique tags with a given frequency. *Green* and *orange* numbers: tags with $P < 0.05$ and $P < 0.01$ for differential expression, respectively. *Green-* and *orange-*numbered tags are differentially expressed according to the test statistic developed by Audic and Claverie.¹⁶ Fifty-four SAGE tags fell outside the 1% confidence interval and 103 fell outside the 5% confidence interval. *Green line:* equal expression between the normal and Fuchs' SAGE libraries. 0 is plotted as 0.5, to be observed on a Log scale.

reproducibility of subpopulations of data from a single SAGE library.¹⁵ In this approach, data sets were generated randomly, keeping the row and column totals of the observed data set fixed. Values were then calculated from each randomly generated data set. This process was repeated 200 times to obtain a distribution of two values under the null hypothesis of no difference between two populations of SAGE data. An empiric probability was calculated by comparing the observed 2 value with the values generated under the null hypothesis. A program was written in a commercial software program (S-Plus 2000; Insightful Corp., Seattle, WA, available at <http://www.insightful.com>) to perform this Monte Carlo simulation and is available on request. The probability for specific pair-wise gene expression differences was calculated using the test statistic developed by Audic and Claverie.¹⁶

SAGE Tag Matching

The ehm-Tag-Mapping method (<http://genome.nhgri.nih.gov/ehm-Tag-Mapping>, provided in the public domain by NHGRI) was used to match SAGE tags with specific UniGene clusters.¹⁵ This method is implemented through the use of several Perl scripts designed to extract tag-to-UniGene cluster information from the UniGene flatfiles available at the National Center for Biotechnology Information (NCBI; <http://www.ncbi.nlm.nih.gov/UniGene>). Briefly, the ehm-Tag-Mapping method extracts a SAGE tag from each sequence in a UniGene cluster, only if the orientation and 3' end of the sequence can be confirmed by identifying poly(A) signals and/or tails. To minimize the extraction of SAGE tags from entries with potential sequencing errors, SAGE tags not representing at least 20% of all tags extracted from a given UniGene cluster are removed from the final ehm-Tag-Mapping flatfile.

Because mitochondrial transcripts are not represented in UniGene, a Perl script was used to extract SAGE tags from a complete annotated

sequence of the human mitochondrial genome (GenBank accession number NC_001807).

RESULTS

Generation of SAGE Data

The SAGE method generates short (10-bp) sequences specific to each expressed gene. In this study, we generated 9,606 SAGE tags from a Fuchs' endothelial SAGE library. A combination of 19,136 tags was analyzed, which includes the 9,530 tags from a previously generated normal corneal endothelial library⁹ (Table 1). This represents only a fraction of the total cloned concatemers in this SAGE library. To minimize the inclusion of SAGE tags arising from sequencing errors, SAGE tag sequences containing *Pbred* scores less than 20 were not added to the database. This resulted in an average *Pbred* score per extracted base of 39, translating to an error rate of 1 in 7943. Because there are 10 bp to a SAGE tag, it can be estimated that approximately 1 in every 794 SAGE tags arose from sequencing errors. The average GC content of the SAGE tags from the normal and Fuchs' SAGE libraries were 51.6% and 51.4%, respectively, indicating that there was no GC content bias during the synthesis of these SAGE libraries.

Using the Monte Carlo simulation approach described in Margulies et al.,¹⁵ each SAGE library was found to be reproducible (Figs. 1A, 1B), indicated by the fact that subpopulations of SAGE data from the same library have observed χ^2 statistics that fall within the null distribution. We were also able to use this method to identify statistically an overall dif-

TABLE 2. SAGE Tags Overexpressed in the Fuchs' Library

| Tag | Normal | Fuchs' | Fold ¹ | P | ID | Description |
|-------------|--------|--------|-------------------|-------|----------|---------------------------------|
| GATCCCAACT | 1 | 11 | 10.9 | 0.004 | 118786 | Metallothionein 2A |
| CTGTTGGTGA | 0 | 7 | 6.9 | 0.009 | 3463 | Ribosomal protein S23 |
| GTGCGGAGGA | 7 | 26 | 3.7 | 0.001 | 332053 | Serum amyloid A1/A2 (Hs.336462) |
| CCCTACCCTG | 68 | 171 | 2.5 | 0.001 | 75736 | Apolipoprotein D |
| CCTGTAATCC | 44 | 133 | 3.0 | 0.001 | 274448 | Hypothetical protein FLJ11029 |
| GTGAAACCCCT | 49 | 110 | 2.2 | 0.001 | 51692 | DKFZP434C091 protein |
| CCTGGCTAAT | 3 | 18 | 6 | 0.001 | 210090 | EST |
| TACCCTAAAA | 11 | 45 | 4.1 | 0.001 | 348470 | EST |
| TTGCCAGGC | 7 | 25 | 3.5 | 0.002 | 271717 | EST |
| GCAAACCCCC | 10 | 35 | 3.5 | 0.001 | 344200 | EST |
| CCTGTAATCC | 44 | 133 | 3 | 0.001 | 345358 | EST |
| TTGGTCAGGC | 15 | 42 | 2.8 | 0.001 | 20996 | EST |
| GTGAAACCCCC | 79 | 182 | 2.3 | 0.001 | 70834 | EST |
| AGGTCAGGAG | 24 | 53 | 2.2 | 0.002 | 344177 | EST |
| TTAGCCAGGA | 2 | 21 | 10.4 | 0.001 | No match | |
| GTGGCGTGCA | 0 | 7 | 6.9 | 0.009 | No match | |
| GTGGCAGGCA | 3 | 17 | 5.6 | 0.002 | No match | |
| TTGGCCAGGC | 31 | 150 | 4.8 | 0.001 | No match | |

Listed are 18 tags over-expressed in the Fuchs' SAGE library, with $P < 0.01$, as determined by the test statistic developed by Audic and Claverie.¹⁶ Fold: the multiple of the difference in abundance of the SAGE tag, which was calculated by dividing the relative abundances in each library. Normal and Fuchs': the number of times the tag was observed in the respective SAGE library. P : for specific pair-wise gene expression differences, the probability was calculated using the test statistic by Audic and Claverie.¹⁶ ID and Description: the human UniGene cluster (Hs.[ID#]) matching a given SAGE tag using the ehm-Tag-Mapping method described in Margulies et al.¹⁵

ference between the normal and Fuchs' SAGE libraries (Fig. 1C), because the observed χ^2 value fell outside the null distribution.

Figure 2 depicts the overall distribution of gene expression between the normal and Fuchs' SAGE libraries, relative to the 1% and 5% confidence intervals from the test statistic developed by Audic and Claverie.¹⁶ Most genes did not have statistically significant probabilities, indicating that the gene expression profiles between these two SAGE libraries were very similar. Also depicted in Figure 2 is the wide range in the levels of gene expression that span more than 2 orders of magnitude, corresponding to a minimum and maximum abundance of 0.01% and 1.96%, respectively. Finally, Figure 2 shows that most of the gene expression complexity (number of unique transcripts) occurred in the lowest abundance class, in agreement with other SAGE experiments¹⁷ as well as earlier nucleic acid reassociation studies,¹⁸ which correlated the reassociation kinetics between mRNA and cDNA molecules with different abundance classes of mRNA.

Identification of Transcripts Overexpressed in Fuchs' Endothelium

Only 18 transcripts demonstrated an increase in expression in Fuchs' endothelium (Table 2). Of these transcripts, six tags identified known genes, eight matched to other ESTs with functions that remain to be determined, and four were novel transcripts exhibiting no similarity to any known sequences.

Identification of Transcripts Underexpressed in Fuchs' Endothelium

The expression of 36 genes was lower in Fuchs' endothelium than in normal endothelium (Table 3). Of these downregulated genes, 26 were known genes, 3 were ESTs, and 7 unknown tags. We found nine different SAGE tags matching mitochondrial sequences, which accounted for 25% of the expressed transcripts that were decreased in Fuchs' endothelium. The remaining 17 underexpressed genes were catalogued according to putative functions (cell division, cell signaling and communication, cell structure and motility, cell and organism de-

fense, gene and protein expression, metabolism, and unclassified), as described by Adams et al.¹⁹ in the Human Genome Project. One underexpressed transcript identified a newly discovered bicarbonate transporter. Decreased transcripts related to antioxidants and proteins conferring protection against toxic stress were noted in Fuchs' versus control subjects including, nuclear ferritin, glutathione *S*-transferase- π , and heat shock 70-kDa protein.

Because the SAGE method is indiscriminate in detecting gene expression in a given tissue, even those not yet identified and cloned, we found that seven downregulated tags did not match any known genes or ESTs and could represent novel genes specific to the corneal endothelium (Table 3). The full SAGE data set can be accessed at the NCBI gene expression Omnibus repository with accession numbers GSM1652 (normal corneal endothelium) and GSM1653 (Fuchs' corneal endothelium).

DISCUSSION

Our data demonstrate the feasibility of applying SAGE for comparison of gene expression between normal and Fuchs' endothelium to identify genes involved in the pathophysiology of the disease. The data revealed that genes regulating cellular energy metabolism, pump functions, and antiapoptotic cell defense dominate the identified transcripts with known functions. These genes may be relevant to the disease process that leads to characteristics of Fuchs' dystrophy, including endothelial decompensation, stromal swelling, corneal guttata, and a thickened Descemet's membrane.

Our data indicate that underexpressed transcripts exceed the overexpressed genes in Fuchs' endothelium. Mitochondrial transcripts account for the majority of these downregulated genes. Mitochondrial genes encode for the enzymes essential for energy metabolism. Our data are consistent with early findings that the numbers of mitochondria and pump site densities are significantly decreased in Fuchs' dystrophy.^{20,21} These data suggest that the basis for endothelial cellular dysfunction is related to energy-dependent activity.

TABLE 3. SAGE Tags Underexpressed in the Fuchs' Library

| Tag | Normal | Fuchs' | Fold | P | ID | Description |
|-------------|--------|--------|------|-------|----------|---|
| CACTACTCAC | 26 | 2 | 13.1 | 0.001 | MITO | Cytochrome <i>b</i> |
| GTGCACGTGAG | 11 | 0 | 11.1 | 0.001 | 181244 | Major histocompatibility complex, class I, A/C (Hs.277477) |
| CTGTACTTGT | 10 | 1 | 10.1 | 0.007 | 75678 | FBJ murine osteosarcoma viral oncogene homolog B |
| GGATATGTGG | 18 | 2 | 9.1 | 0.001 | 326035 | Early growth response 1 |
| ACCCTTGGCC | 21 | 3 | 7.1 | 0.001 | MITO | NADH dehydrogenase subunit 1 |
| ACTGGGTCTA | 7 | 0 | 7.1 | 0.008 | 275163 | Nonmetastatic cells 2, protein (NM23B) expressed in |
| AGGTCTGCCA | 7 | 0 | 7.1 | 0.008 | 201967 | Aldo-keto reductase family 1, member C2 |
| GCGCTGGAGT | 7 | 0 | 7.1 | 0.008 | 110695 | Hypothetical protein MGC3133 |
| AGGTCCTAGC | 16 | 3 | 5.4 | 0.003 | 226795 | Glutathione S-transferase pi |
| GCTGACTCAG | 20 | 4 | 5 | 0.001 | 105607 | Bicarbonate transporter related protein 1 |
| ACTAACACCC | 23 | 5 | 4.6 | 0.001 | MITO | NADH dehydrogenase subunit 2 |
| TCCATCTGGT | 21 | 5 | 4.2 | 0.002 | 75410 | Heat shock 70kD protein 5 (glucose-regulated protein, 78kD) |
| TGATTTCACT | 27 | 7 | 3.9 | 0.001 | MITO | Cytochrome <i>c</i> oxidase subunit III |
| CAGGTTTCAT | 19 | 5 | 3.8 | 0.004 | 24395 | Small inducible cytokine subfamily B (Cys-X-Cys), member 14 |
| GTAAGTGTAC | 102 | 31 | 3.3 | 0.001 | MITO | 12S ribosomal RNA |
| AGAAAGATGT | 21 | 7 | 3 | 0.008 | 78225 | Annexin A1 |
| TTGGTCTTTG | 48 | 18 | 2.7 | 0.001 | 66739 | Keratin 12 (Meesmann corneal dystrophy) |
| CACCTAATTG | 119 | 50 | 2.4 | 0.001 | MITO | ATP synthase F0 subunit 6 |
| CCCATCGTCC | 187 | 77 | 2.4 | 0.001 | MITO | Cytochrome <i>c</i> oxidase subunit II |
| TTCATACACC | 46 | 20 | 2.3 | 0.002 | MITO | NADH dehydrogenase subunit 4 |
| CTAAGACTTC | 74 | 35 | 2.1 | 0.001 | MITO | 16S ribosomal RNA |
| GGCCCAGGCC | 71 | 34 | 2.1 | 0.001 | 575 | Aldehyde dehydrogenase 3 family, member A1 |
| TACCATCAAT | 59 | 28 | 2.1 | 0.001 | 169476 | Glyceraldehyde-3-phosphate dehydrogenase |
| TGTGTTGAGA | 45 | 23 | 2 | 0.007 | 288036 | tRNA isopentenylpyrophosphate transferase |
| GCCCCTGCTG | 54 | 28 | 1.9 | 0.004 | 195850 | Keratin 5 |
| TTGGGGTTTC | 98 | 62 | 1.6 | 0.004 | 62954 | Ferritin, heavy polypeptide 1 |
| GGTCACTGAG | 12 | 2 | 6 | 0.008 | 347378 | EST |
| GCAAGCCAAC | 16 | 4 | 4 | 0.007 | 332048 | EST |
| CTCATAAGGA | 52 | 15 | 3.5 | 0.001 | 294348 | EST |
| ACACAGCAAG | 22 | 1 | 22.2 | 0.001 | No match | |
| GGGAAGCAGA | 53 | 7 | 7.6 | 0.001 | No match | |
| GAAGTCGGAA | 14 | 2 | 7.1 | 0.003 | No match | |
| AGTAGGTGCG | 13 | 2 | 6.6 | 0.004 | No match | |
| GCTTTCTCAC | 35 | 6 | 5.9 | 0.001 | No match | |
| AAAACATTCT | 25 | 5 | 5 | 0.001 | No match | |
| CAAGCATCCC | 34 | 12 | 2.9 | 0.001 | No match | |

Listed are 36 tags underexpressed in the Fuchs' library, with $P < 0.01$, as determined by the test statistic developed by Audic and Claverie.¹⁶ See Table 1 for column descriptions. MITO refers to tags that match mitochondrial transcripts.

Mitochondria are the major source of cellular reactive oxygen species (ROS). Mitochondrial DNA (mtDNA) is especially vulnerable to oxidative damage because of its proximity to the inner mitochondrial membrane, where electron transport systems generate ROS. Recent evidence indicates that oxidative DNA damage is a major cause of aging.²² A number of age-related neuromuscular degenerative diseases have been associated with point mutations and deletions in mtDNA, and progressive accumulation over time of oxidative damage in mtDNA from neuronal tissues has been demonstrated.²³ Fuchs' dystrophy is a progressive disease that does not manifest clinically until the third or fourth decade.¹ Gradual oxidative mtDNA damage may occur over time in Fuchs' endothelial cells. The progressive oxidative damage would probably increase the number of mtDNA mutations, which would eventually interfere with polypeptides encoded by mutated genes and lead to a degradation in enzyme activity. Biochemical findings that support this hypothesis include the demonstration that respiratory enzyme complexes gradually decline in Fuchs' endothelial cells.^{22,23} In addition, a patient with Fuchs' dystrophy has been reported to have missense mutations in the mtDNA at position 15,257 of the cytochrome *b* subunit of complex III and at position 4213 of the ND1 subunit of complex I.²⁴ However, further study is necessary to determine whether mitochondrial defects could be the root cause of this dystrophy.

The endothelial pump is an essential requirement for maintaining proper fluid transport and hydration in the cornea. Na^+ , K^+ , ATPase has been identified as an important pump in

the endothelial plasma membrane requiring adenosine triphosphate (ATP). SAGE has identified several Na^+ , K^+ , ATPases.⁹ Although comparisons of SAGE Fuchs' versus normal endothelial transcripts did not show a significant difference between the Na^+ , K^+ , ATPases of the two libraries, the substantial decrease in other mitochondrial gene transcripts may have compromised ATP production to such a low level that proper Na^+ , K^+ pump function could not be maintained. A comparison of the two libraries revealed a significant decrease in the expression of a newly reported bicarbonate transporter, bicarbonate transporter-related protein-1 (BTR1).²⁵ Although the precise transport activity of BTR1 is yet to be determined, this bicarbonate transporter is believed to be responsible for as yet unexplained anion transport identified in several human tissues including the kidney and salivary glands.

There are many ways to activate apoptosis in a cell, but in general two main pathways predominate: an intrinsic pathway involving mitochondria and an extrinsic pathway initiated by cell surface receptors for growth factors, cytokines, or drugs.²⁶ Apoptosis has been shown to play a role in endothelial cell death in Fuchs' dystrophy.²⁷ Which apoptotic pathway is executed in endothelial cell death in Fuchs' dystrophy is not known, but our data favor the intrinsic pathway. Mitochondria play a central role in apoptosis, as cytochrome *c* released in the cytoplasm opens permeability transition pores and leads to the apoptotic cascade.²⁸ The sensitive balance between ROS production and antioxidant defenses determines the degree of oxidative stress. Consequences of this stress include modification of cellular proteins, lipids, and DNA that could result in

cell death. Our data indicate that Fuchs' endothelial cells exhibit decreased abundance of transcripts related to antioxidants and proteins conferring protection against toxic stress. For examples, nuclear ferritin protects DNA against UV damage.²⁹ Glutathione S-transferase- π catalyzes intracellular detoxification reactions by conjugating glutathione with electrophilic compounds resulting in the elimination of toxic compounds.^{30,31} Heat shock 70-kDa protein is a major cytoplasmic chaperone that protects cells against apoptosis.³² Downregulation of these genes may in turn increase the production of ROS and toxic molecules that may have an especially detrimental impact, because corneal endothelial cells are terminally differentiated and will not be replaced.

Apolipoprotein D (apoD) is a lipophilic protein that has an important function in nerve regeneration. A large increase of apoD concentration has been found in the cerebrospinal fluid of patients with Alzheimer's disease and other neuropathologic conditions.³³ Our study shows that ApoD gene is expressed at moderate level in normal endothelium, but its expression markedly increases in Fuchs' dystrophy. Overexpression of apoD may represent tissue injury repair in Fuchs' dystrophy. An unexpected result was the differences in transcript abundance among the ribosomal proteins between normal and Fuchs' endothelium.

Our observation that 11 differentially expressed SAGE tags do not match any known sequences suggests that a number of human genes may remain untagged, despite the large number of SAGE tags currently available and despite the data in the Human Genome Project. These no-match tags may represent novel genes putatively involved in maintaining endothelial functions and may provide insight into essential missing links in the molecular pathogenic pathways of Fuchs' dystrophy. Furthermore, these no-match tags sequences can be used to further identify the corresponding uncharacterized genes.

In summary, we have applied SAGE technology to identify differentially expressed tags corresponding to known and unknown genes possibly involved in the pathophysiology of Fuchs' dystrophy. At least three possible roles for these differentially expressed genes in this endothelial degeneration may be hypothesized: diminished pump function capacity due to under expression of key transporter components and/or decreased mitochondrial delivery of adequate energy sources to maintain pump; an apoptotic cascade of events leading to endothelial cell death as a result of oxidative stress, mitochondrial damage, and/or diminished levels of antioxidants; and overexpression of defensive genes to inhibit apoptosis. Our study demonstrates that analysis of global gene expression profiles can identify a group of genes that function in a common pathway to illuminate the underlying mechanism of a complex disease process in Fuchs' dystrophy.

References

1. Wilson SE, Bourne WM. Fuchs' dystrophy. *Cornea*. 1988;7:2-18.
2. Adamis AP, Filatov V, Tripathi BJ, Tripathi RC. Fuchs' endothelial dystrophy of the cornea. *Surv Ophthalmol*. 1993;38:149-168.
3. Cross HE, Maumenee AE, Cantolino SJ. Inheritance of Fuchs' endothelial dystrophy. *Arch Ophthalmol*. 1971;85:268-272.
4. Magovern M, Beauchamp McTigue JW, Baumiller RC. Inheritance of Fuchs' combined dystrophy. *Ophthalmology*. 1979;86:1897-1923.
5. Rosenblum P, Stark WJ, Maumenee IH, Hirst LW, Maumenee AE. Hereditary Fuchs' dystrophy. *Am J Ophthalmol*. 1980;90:455-462.
6. Lipshutz RJ, Fodor SP, Gingeras TR, Lockhart DJ. High density synthetic oligonucleotide arrays. *Nat Genet*. 1999;21(suppl):20-24.
7. Duggan DJ, Bittner M, Chen Y, Meltzer P, Trent JM. Expression profiling using cDNA microarrays. *Nat Genet*. 1999;21(suppl):10-14.
8. Velculescu VE, Zhang L, Vogelstein B, Kinzler KW. Serial analysis of gene expression. *Science*. 1995;270:484-487.
9. Gottsch JD, Seitzman G, Margulies EH, et al. Gene expression in donor corneal endothelium *Arch Ophthalmol*. In press.
10. St Croix B, Rago C, Velculescu V, et al. Genes expressed in human tumor endothelium. *Science* 2000;289:1192-1202.
11. Ewing B, Hillier L, Wendl MC, Green P. Base-calling of automated sequencer traces using *Pbred*. I: accuracy assessment. *Genome Res*. 1998;8:175-185.
12. Margulies EH, Innis JW. eSAGE: managing and analysing data generated with serial analysis of gene expression (SAGE). *Bioinformatics*. 2000;16:650-651.
13. Margulies EH, Kardia SLR, Innis JW. Identification and prevention of a GC content bias in SAGE libraries. *Nucleic Acids Res*. 2001;29:E60.
14. Sokal RR, Rohlf FJ. *Biometry: The Principles and Practice of Statistics in Biological Research*. 3rd ed. New York: Freeman; 1995.
15. Margulies EH, Kardia SLR, Innis JW. A comparative molecular analysis of developing mouse forelimbs and hindlimbs using serial analysis of gene expression (SAGE). *Genome Res*. 2001;11:1686-1698.
16. Audic S, Claverie JM. The significance of digital gene expression profiles. *Genome Res*. 1997;7:986-995.
17. Zhang L, Zhou W, Velculescu VE, et al. Gene expression profiles in normal and cancer cells. *Science*. 1997;276:1268-1272.
18. Hastie ND, Bishop JO. The expression of three abundance classes of messenger RNA in mouse tissues. *Cell*. 1976;9:761-774.
19. Adams MD, Kerlavage AR, Fleischmann RD, et al. Initial assessment of human gene diversity and expression patterns based upon 83 million nucleotides of cDNA sequence. *Nature*. 1995;377(suppl):3-174.
20. Tuberville AW, Wood TO, McLaughlin BJ. Cytochrome oxidase activity of Fuchs' endothelial dystrophy. *Curr Eye Res*. 1986;5:939-947.
21. McCartney MD, Wood TO, McLaughlin BJ. Moderate Fuchs' endothelial dystrophy ATPase pump site density. *Invest Ophthalmol Vis Sci*. 1989;30:1560-1564.
22. Finkel T, Holbrook NJ. Oxidant, oxidative stress and the biology of ageing. *Nature*. 2000;408:239-245.
23. Wallace DC. Diseases of the mitochondrial DNA. *Annu Rev Biochem*. 1992;61:1175-1212.
24. Albin RL. Fuchs' corneal dystrophy in a patient with mitochondrial DNA mutations. *J Med Genet*. 1998;35:258-259.
25. Parker MD, Ourmozdi EP, Tanner MJA. Human BTR1, a new bicarbonate transporter superfamily member and human AE4 from kidney. *Biochem Biophys Res Commun* 2001;282:1103-1109.
26. Kroemer G, Zamzami N, Susin SA. Mitochondrial control of apoptosis. *Immunol Today*. 1997;18:44-51.
27. Borderie VM, Baudrimont M, Vallee A, Ereau TL, Gray F, Laroche L. Corneal endothelial cell apoptosis in patients with Fuchs' dystrophy. *Invest Ophthalmol Vis Sci*. 2000;41:2501-2505.
28. Korsmeyer SL. Regulators of cell death. *Trends Genet*. 1995;11:101-105.
29. Cai CX, Birk DE, Linsenmayer TF. Nuclear ferritin protects DNA from UV damage in corneal epithelial cells. *Mol Biol of the Cell*. 1998;9:1037-1051.
30. Brigelius-Flohe R. Tissue-specific functions of individual glutathione peroxidases. *Free Radic Biol Med*. 1999;27:951-965.
31. Mannervik B. The isoenzymes of glutathione S-transferase. *Adv Enzymol*. 1985;57:357-417.
32. Jolly C, Morimoto RI. Role of the heat shock response and molecular chaperones in oncogenesis and cell death. *J Natl Cancer Inst*. 2000;92:1564-1572.
33. Terrisse L, Poirier J, Bertrand P, et al. Increased levels of apolipoprotein D in cerebrospinal fluid and hippocampus of Alzheimer's patients. *J Neurochem*. 1998;71:1643-1650.